Large-scale carbon isotope fractionation in evaporites and the generation of extremely ^{13}C-enriched methane

Joanna Potter*
Michael G. Siemann
Institut für Mineralogie und Mineralische Rohstoffe, Technische Universität Clausthal, Adolph-Roemer Strasse 2a, 38678 Clausthal-Zellerfeld, Germany
Mikhail Tsypukov Institut für Mineralogie und Mineralische Rohstoffe, Technische Universität Clausthal, Adolph-Roemer Strasse 2a, 38678 Clausthal-Zellerfeld, Germany, and Institute of Geochemistry, Russian Academy of Science, Irkutsk, Russia

ABSTRACT

Petrographic, fluid-inclusion, geochemical, and gas stable isotope data are reported here for a Permian Zechstein evaporite sequence. This deposit is a geochemically unaltered sequence. Bromine concentrations show a continuous evaporation profile with little postdepositional alteration in halite chemistry. Bacterial fermentation gases, identified in primary inclusions, change from an N_2-H_2S composition in the lower-middle halite series to a CH_4-H_2 composition in the upper halite and potash series. Carbon isotope results for CH_4 show a ^{13}C enrichment up-sequence from typical biogenic values of −45‰ to −50‰ to extremely unusual ^{13}C-enriched values as high as +21‰. The δD values for these ^{13}C-enriched CH_4 gases range from −240‰ to −377‰. A model is proposed for the formation of the CH_4 gases whereby the dominant isotopic fractionation process controlling the system was evaporation of the brines. This generated a progressive ^{13}C enrichment in the carbon in the residual brines due to preferential loss of $^{12}CO_2$ to the atmosphere. The resulting CH_4 generated in the sediments, as evaporation and precipitation advanced, recorded this ^{13}C enrichment in the carbon reservoir. Therefore, the isotopic profile observed in this sequence today represents a primary feature with little evidence for postdepositional migration.

Keywords: methane, evaporites, stable isotopes, fluid inclusions.

INTRODUCTION

Evaporites host a variety of gaseous species. Studies have reported gas assemblages such as N_2-O_2 mixtures, interpreted as atmospheric in origin (Freyer, 1978; Siemann and Ellendorff, 2001); N_2-CH_4 mixtures, interpreted as biogenic products (Nesmelova and Travnikova, 1973; Freyer, 1978; Grishina et al., 1998; Siemann and Ellendorff, 2001); oil- and CO_2-rich inclusions, interpreted to have been generated either in situ or by migration from underlying source rocks (e.g., Pironon et al., 1995), or from thermal alteration of mineral and gas phases by igneous intrusions (e.g., Grishina et al., 1992); and CH_4-N_2-H_2-H_2S gas mixtures in which H_2 has been attributed to radiogenic and/or biogenic reactions (Nesmelova and Travnikova, 1973; Gerling et al., 1988; Siemann and Ellendorff, 2001).

As these reports show, it is important to understand the history of an evaporite sequence in order to interpret the origin and subsequent behavior of gases within the sequence. This is only possible by carrying out a comprehensive petrographic, geochemical, and isotopic study on the evaporite deposit in question. Results of such a study are reported here for a Permian sequence. These results include the discovery of extremely unusual ^{13}C-enriched CH_4 hosted in the deposit.

GEOLOGIC SETTING

A 200 m drill core through a Zechstein 2 evaporite cycle was collected from the Zielitz mine, near Magdeburg, northeast Germany. The sequence was taken from the Stassfurt series (Z2) in the Scholle von Calvörde region, part of the larger Permian Zechstein Basin (ca. 255–256 Ma). This deposit has been subjected to little tectonic activity. The core starts at the basal anhydrite (z2ANa) and goes up through the main halite series (z2Na) into the potash series (z2KSt). The halite series is homogeneous with no distinguishable subseries and is ~60 m in true thickness. The potash series consists of a primary potassium-bearing mineral assemblage of carnallite, kieserite, and halite.

ANALYTICAL METHODS

The study was divided into four phases. The first phase was to analyze the gases trapped between the grains (referred to as grain-boundary gases). Samples of 15 cm core were taken every 2 m and sealed in gas-tight bags that were subsequently evacuated. The samples were then lightly crushed to release the grain-boundary gases. The resultant crushed fraction ranged between 1 and 5 cm, leaving intragranular inclusions intact. The released gases were transferred by gas-tight syringe to a ThermoFinnigan gas chromatograph–isotope-ratio mass spectrometer for COHN stable isotope analysis (see Potter and Siemann, 2004, for technical details). All $\delta^{13}C$ values reported are referenced to Vienna Peedee belemnite (VPDB), δD and $\delta^{18}O$ values are referenced to Vienna standard mean ocean water (VSMOW), and $\delta^{15}N$ is referenced to air-N_2. The second phase was to obtain Br concentrations on mineral separates from the samples to get a geochemical profile of the evaporite sequence. The samples were crushed into millimeter-sized crystals and washed with deionized water to remove any surficial brine. The samples were then cleaned with pure ethanol and dried in an oven before dissolution. Bromine concentrations were measured with a Metrohm ion-chromatograph (see Siemann and Schramm, 2002). The third phase was a fluid-inclusion study. Petrographic and laser-Raman microprobe studies on prepared wafers identified inclusion populations and gas phases present as grain-boundary and intragranular inclusions. A Dilor laser-Raman microprobe with a Nd-YAG laser (532 nm) allowed identification of the volatiles within the fluid inclusions. For the final phase, the crystals hosting primary fluid inclusions were separated out and dissolved; the gases were extracted for isotopic evaluation in order to ascertain if there were any differences between these and the grain-boundary gases (the results are briefly discussed here).

RESULTS

Petrographic and Fluid-Inclusion Results

Figure 1 shows the stratigraphic and petrographic features of this sequence along with the geochemical and isotopic results. The main halite series (z2Na) shows petrographic features typical of a buried evaporite sequence (cf. Roedder, 1984). Most of the halite shows localized recrystallization to clear halite with a low abundance of fluid inclusions. Inclusions in these recrystallized zones occur as secondary trails of brine and vapor. However, areas with primary, cloudy halite can be found throughout the sequence, increasingly toward the top of the halite series. At the top of the series, chevron structures are commonly observed. The primary inclusions in these chevrons (Fig. 2A) and clouds (Fig. 2B) are composed of brine ± gas ± solids. The

*E-mail: joanna.potter@tu-clausthal.de.

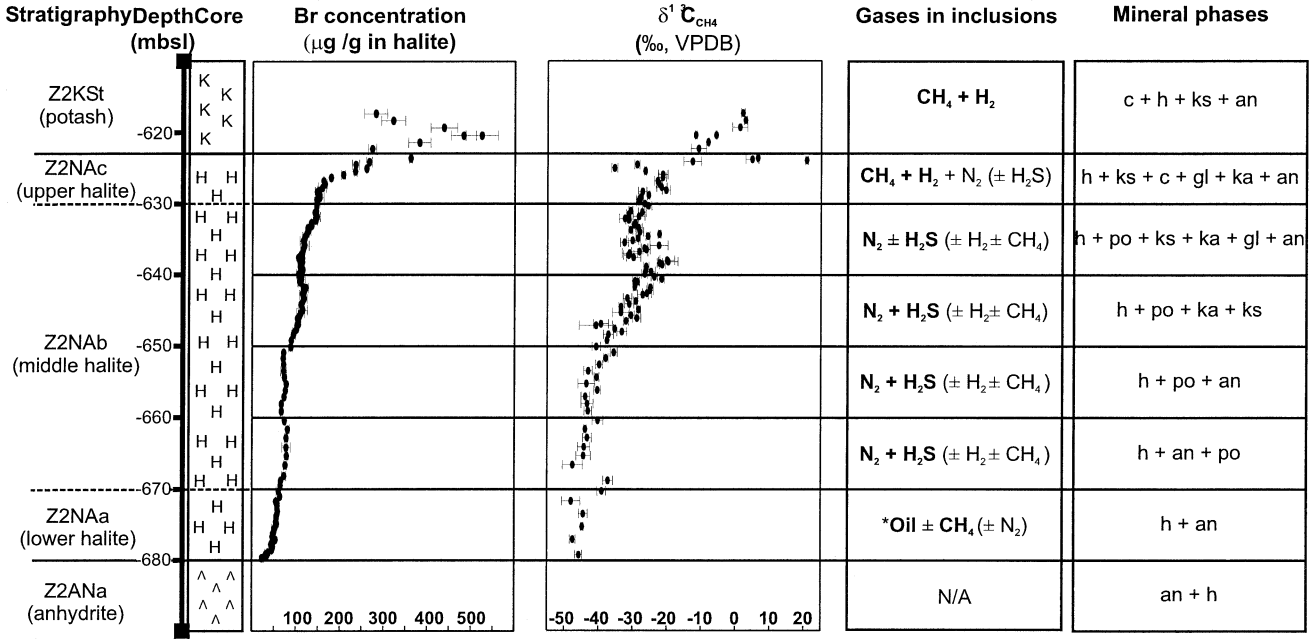

Figure 1. Summary of features in this Zechstein sequence with results from bromine analyses, CH_4 carbon isotope results for grain-boundary gases and gas phases in primary inclusions. Divisions of Zechstein series are shown at left; mbsl—meters below sea level. Parentheses indicate trace gas phases, asterisks indicate secondary inclusions. Mineral phases: an—anhydrite ($CaSO_4$), h—halite (NaCl), po—polyhalite [$K_2MgCa_2(SO_4)4{\cdot}2H_2O$], ka—kainite ($KMgClSO_4{\cdot}2.75H_2O$), ks—kieserite ($MgSO_4{\cdot}H_2O$), gl—glauberite [$Na_2Ca(SO_4)_2$], c—carnallite ($KMgCl_3{\cdot}6H_2O$), VPDB—Vienna Peedee belemnite.

heterogeneity of the phases in these inclusions may indicate necking down and remobilization of the inclusion phases in the individual crystals upon burial. Minor phases present as solid inclusions in the halite can be found throughout the halite series. These show an evolution in the mineral assemblage up-sequence from anhydrite and polyhalite to kieserite and carnallite (e.g., Figs. 2C and 2D). These solids have brine or gas inclusions associated with them, trapped between the solid inclusion and host halite (Figs. 2C and 2D). The concentration of fluid inclusions around these solid inclusions is thought to be due to low-energy nucleation sites at the solid inclusion surfaces, promoting the formation of inclusions at these sites during crystallization (Roedder, 1984). The solid inclusions are thought to be primary, with the exception of anhydrite, which recrystallized from gypsum. The fluid inclusions associated with these solids are therefore considered to represent primary fluids. The potash series contains abundant small primary gas inclusions (Fig. 2E) that are dispersed in bands throughout the host mineral lattice (e.g., carnallite). The gases detected in these primary inclusions change up-sequence from N_2-H_2S gases to CH_4-H_2 gases (Fig. 1). Abundant secondary trails of inclusions of oil and CH_4 are found at the base of the halite (Fig. 2F).

Br Concentrations in the Evaporite

The Br concentrations (Fig. 1) show a typical profile for a primary evaporite sequence (cf. Braitsch, 1971; Siemann, 2003). Concentrations of ~50 μg Br/g halite are average at the onset of halite precipitation; the concentrations increase to 300 μg Br/g halite at the top of the halite series. The potash salts have concentrations between 300 and 600 μg Br/g halite. This profile shows no evidence for a complex depositional history or Br migration due to postdepositional recrystallization (cf. Braitsch, 1971; Sonnenfeld, 1984). The exception is at the base of the halite, where the Br concentrations are anomalously low (to 20 μg Br/g).

Stable Isotope Results for the Grain-Boundary Gases

Gases from the crushed cores consisted of CH_4, H_2, N_2, and O_2. The N_2 and O_2 are interpreted to be atmospheric contaminants; $\delta^{15}N$ ranged between −0.02‰ and +0.61‰ and $\delta^{18}O$ ranged between +23.50‰ and +23.94‰. Significant amounts of H_2 were detected in the potash samples. The δD_{H_2} for these samples ranged between −667‰ and −719‰, typical for H_2 formed at low temperatures (Bottinga, 1969). CH_4 was detected throughout the sequence. High volumes of CH_4 were released at the base and the top of the halite. Trace amounts of CH_4 were released from the middle of the halite. The $\delta^{13}C_{CH_4}$ values were obtained for the whole sequence, but δD_{CH_4} values were only determined for samples with large volumes of CH_4. Figure 1 shows the $\delta^{13}C_{CH_4}$ profile through the sequence. It is apparent that there is an increase in $\delta^{13}C_{CH_4}$ up-sequence, starting at values of −45‰ to −50‰ and increasing to ^{13}C-enriched values (to +21‰) at the top.

Figure 3 shows results of δD and $\delta^{13}C$ determined for the CH_4 at the base of the halite, the top of the halite, and in the potash series. It is evident that there are two sources of CH_4 in this sequence. At the base of the halite, the CH_4 has a typical thermogenic signature, whereas at the top of the sequence, the CH_4 has lower δD and higher $\delta^{13}C$ values, falling outside of any defined source field. Therefore, these gases were modified by some type of fractionation process that shifted the isotopic values away from typical CH_4 values.

ORIGIN OF CH_4 AND OTHER GASES IN THE EVAPORITE SEQUENCE

The two different sources of CH_4 distinguished in the stable isotope results for the grain-boundary gases are supported by fluid-inclusion observations. The CH_4 found in inclusions at the base of the halite is associated with grain boundaries and included secondary trails of oil (Fig. 2F), confirming a thermogenic origin for both the grain-boundary and included CH_4. This indicates that some oil generation or migration occurred at the base of the halite and explains the low Br concentrations observed due to leaching of Br from the halite during interaction with the oil-bearing fluids (Fig. 1). The oil is restricted to the base of the halite; there is little evidence of migration into the rest of the sequence. The gases present abruptly change to an $N_2 + H_2S \pm H_2 \pm CH_4$ assemblage, which is found in primary inclusions. This

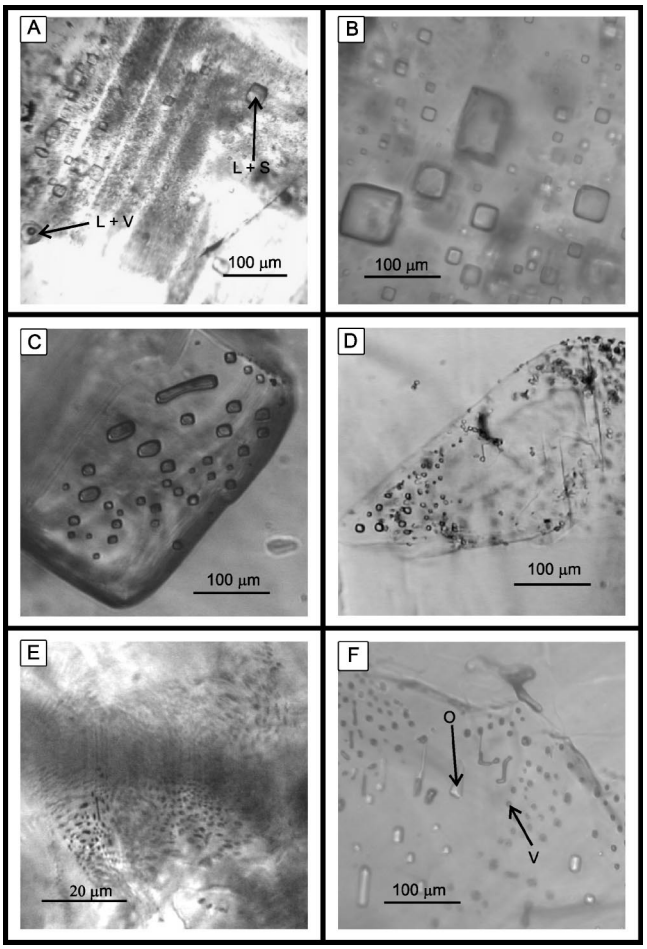

Figure 2. A: Primary chevron structures in halite containing inclusions of brine (L), gas (V), and solids (S) (upper halite). B: Clouds of primary brine inclusions (middle-upper halite). C: Solid inclusion of polyhalite with gas inclusions (middle halite). D: Solid inclusion of anhydrite with gas or liquid inclusions on crystal surfaces (middle halite). E: Gas inclusions in carnallite (potash). F: Secondary oil (O) and gas (V) inclusions in trails and along grain boundaries (base of halite sequence).

changes at the top of the halite series to a $CH_4 + H_2 \pm H_2S \pm N_2$ assemblage (Fig. 1). Preliminary $\delta^{13}C$ analyses on CH_4 extracted from these primary inclusions give either the same result or are slightly lower than results from the grain-boundary CH_4. This indicates that the CH_4 trapped at both the grain boundaries and in inclusions in the middle and upper halite and potash series have a common source. CH_4 that is not associated with oil can be generated through two reaction pathways, CO_2 reduction or bacterial fermentation (e.g., Whiticar et al., 1986). The CO_2 reduction consumes H_2, generating CH_4 and H_2O, whereas bacterial fermentation reactions produce a range of gases such as CH_4, H_2S, N_2, CO_2, and H_2. The primary gas assemblage found in this sequence, therefore, would favor a bacterial fermentation origin. An N_2-H_2S assemblage in the middle halite suggests that denitrification and sulfate reduction reactions were dominant. As conditions became more reducing and sulfate availability decreased with progressive evaporation, methanogenic reactions became dominant with a change to a CH_4-H_2 gas assemblage (e.g., Oremland and Taylor, 1978; Whiticar et al., 1986). Such conditions can exist at depth and in sediments as hypersaline anaerobic brines with Eh as low as −600 mV (Sonnenfeld, 1984).

The δD_{CH_4} values recorded for CH_4 at the top of the halite and in the potash series (−370‰ to −240‰) also favor a bacterial fermentation origin. Assuming an initial δD_{H_2O} value of 0‰ for typical

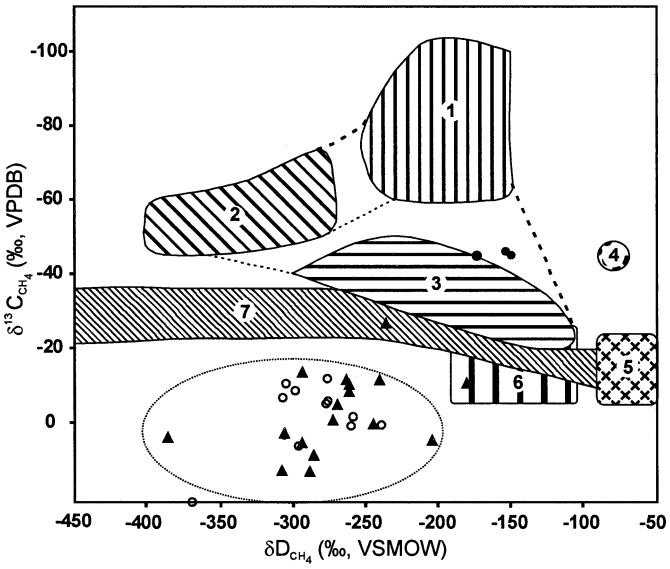

Figure 3. $\delta^{13}C$ vs. δD data for CH_4. Solid dots—lower halite series; open circles—upper halite and potash series (data from this study), triangles—data from Zechstein 2 potash deposits (Gerling et al., 1988). CH_4 source fields (based on Schoell, 1988): 1—CO_2 reduction, 2—bacterial fermentation, 3—thermogenic, 4—atmosphere, 5—mantle, 6—abiogenic, 7—hot springs. VPDB—Vienna Peedee belemnite. VSMOW—Vienna standard mean ocean water.

seawater and applying fractionation factors for acetate fermentation and CO_2 reduction reported by Whiticar et al. (1986), the resulting δD_{CH_4} values would be between −370‰ and −450‰ for fermentation and between −160‰ and −200‰ for CO_2 reduction. This would indicate that acetate fermentation was the main CH_4 generating pathway.

To produce the ^{13}C-enriched CH_4, a further fractionation process must have played a role in altering these gases. Earlier reports identified ^{13}C-enriched carbon species, the most common being enriched CO_2 and carbonates, as a product of fermentation reactions where the oxidized carbon species is preferentially enriched in CH_4 (e.g., Dimitrakopoulos and Muehlenbachs, 1987). This does not explain the ^{13}C-enriched CH_4 in this study. The ^{13}C-enriched CH_4 can be a residual product of microbial oxidation reactions generating light CO_2 (e.g., Coleman et al., 1981). However, the reduced gas assemblage in this sequence precludes this as a valid pathway. Therefore, in order to explain the formation of ^{13}C-enriched CH_4 in this sequence, these results can instead be compared to similar results from other evaporite environments. Gerling et al. (1988) reported $\delta^{13}C_{CH_4}$ values to +13‰ in similar potash deposits (Fig. 3). Stiller et al. (1985) reported $\delta^{13}C_{CO_2}$ values to +16.5‰ for ΣCO_2 dissolved in solar brine pools, and Clark and Lauriol (1992) investigated the formation of ^{13}C-enriched calcites (to +17‰) in karstic caves in the Yukon, Canada. All these environments have precipitates forming in evaporative conditions, suggesting that the evaporative process is the key factor.

Therefore, the ^{13}C enrichment observed in the grain-boundary (and included) CH_4 gases could represent the carbon isotopic evolution of an evaporating basin. A model is proposed where the basin essentially acted as a closed body of water in which light CO_2 degassed and was removed from the system. As the salts were deposited, interstitial anoxic waters were trapped and CH_4 was generated. Rapid cementation of the salts must have occurred, effectively isolating the entrapped gases and allowing no further interaction with the evolving brines, thus preserving the carbon isotopic profile observed today. The presence of H_2 in the upper halite and potash series supports the assumption that these salts have remained closed.

A theoretical Rayleigh kinetic fractionation model can be applied

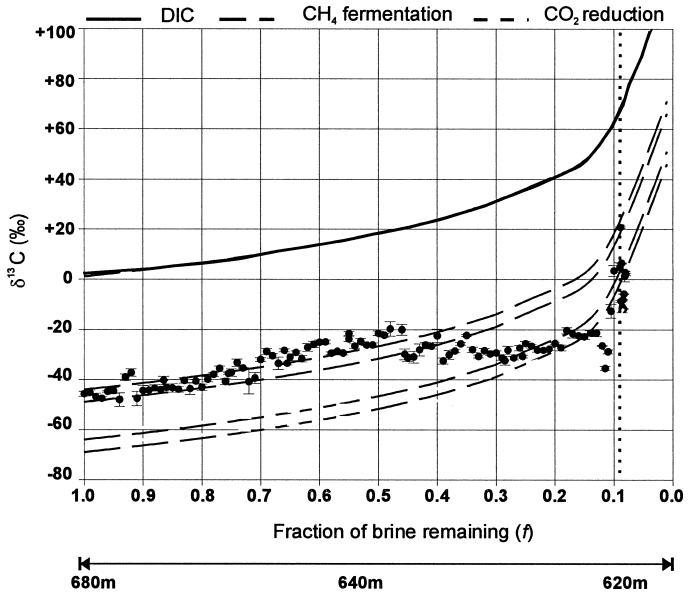

Figure 4. Model showing calculated $\delta^{13}C$ values for dissolved inorganic carbon (DIC) and CH_4 in progressively evaporating basin. Fractionation model data: $\delta f = \{[(\alpha - 1) \times 10^3]\ln f\} + \delta o$. $\delta f = \delta$ value at remaining fraction (f), δo = initial δ value, kinetic fractionation factor $\alpha_{KIE} = 1.025$, fractionation factors from DIC to CH_4 generated by fermentation (ferm) and CO_2 reduction reactions (red): $\alpha_{CH_4ferm-DIC} = 1.045–1.05$ and $\alpha_{CH_4red-DIC} = 1.065–1.07$ (Whiticar et al., 1986; Clark and Fritz, 1997). $\delta^{13}C_{CH_4}$ and associated depth data from Figure 1 are superimposed for comparison.

to test this hypothesis. Stiller et al. (1985) calculated a kinetic fractionation (α_{KIE}) for the solar brine pools at 45 °C (1.02), similar to the fractionation calculated by Clark and Lauriol (1992) for the cryogenic calcites at 0 °C (1.03). Therefore, in this model a fractionation of 1.025 is used, assuming temperatures were between 20 and 30 °C. Taking an initial $\delta^{13}C_{DIC}$ value of +1‰, based on typical seawater equilibrium compositions (Mook, 2001), the incremental $\delta^{13}C_{DIC}$ values of an evaporating body can be calculated (Fig. 4). For the resulting $\delta^{13}C_{DIC}$, there is a progressive enrichment of ^{13}C to values of +100‰ at the end of evaporation. Assuming that the dissolved inorganic carbon (DIC) was eventually converted to CH_4 within the sediments, the fractionation factors between $\delta^{13}C_{DIC}$ and $\delta^{13}C_{CH_4}$ for fermentation and CO_2 reduction (Whiticar et al., 1986; Clark and Fritz, 1997) can be applied to this fractionation curve (Fig. 4). The modeled $\delta^{13}C_{CH_4}$ results for fermentation follow a trend similar to the CH_4 results in the evaporite sequence, starting at initial values of ~−45‰ and increasing to >+20‰ at >95% evaporation. At the top of the sequence, CO_2 reduction may have started to play a role in generating CH_4, with a departure from the fermentation curve and interception with the predicted CO_2 reduction curve. Carnallite saturation is reached in an evaporating solution at $f = 0.09$ (Fig. 4). On the $\delta^{13}C_{CH_4}$ fermentation curve, this corresponds to values between +13‰ and +17‰, and on the CO_2 reduction curve, it corresponds to between −7‰ and −2‰, well within the range of $\delta^{13}C_{CH_4}$ values found in the samples from the top of the halite and from the potash series.

CONCLUSIONS

The dominant gas assemblage formed within the sediment substrate in this untectonized evaporite sequence consists predominantly of bacterial fermentation gases. CH_4 is the dominant carbon gas species and shows progressive ^{13}C enrichment up-sequence toward unusually high $\delta^{13}C$ values, out of any previously defined source fields. These values can be explained by a kinetic fractionation model for an evaporating water body with progressive enrichment of ^{13}C in the residual brines during evaporation. This enrichment has been retained in CH_4 found in primary fluid inclusions and along grain boundaries.

ACKNOWLEDGMENTS

This study was financed by the R + D Program Management "Water Technology and Disposal" (02 C 0851) of the Federal Ministry of Education, Science, Research and Technology (BMBF/PTE). We thank Tony Fallick, Russell Shapiro, and an anonymous reviewer for helpful reviews that improved the manuscript.

REFERENCES CITED

Bottinga, Y., 1969, Calculated fractionation factors for carbon and hydrogen isotope exchange in the system calcite–carbon dioxide–graphite–methane–hydrogen–water vapour: Geochimica et Cosmochimica Acta, v. 33, p. 49–64.

Braitsch, O., 1971, Salt deposits: Their origin and composition: Berlin, Springer-Verlag, 297 p.

Clark, I.D., and Fritz, P., 1997, Environmental isotopes in hydrogeology: Boca Raton, Florida, Lewis Publishers, 350 p.

Clark, I.D., and Lauriol, B., 1992, Kinetic enrichment of stable isotopes in cryogenic calcites: Chemical Geology, v. 102, p. 217–228.

Coleman, D.D., Risatti, J.B., and Schoell, M., 1981, Fractionation of carbon and hydrogen isotopes by methane-oxidizing bacteria: Geochimica et Cosmochimica Acta, v. 45, p. 1033–1037.

Dimitrakopoulos, R., and Muehlenbachs, K., 1987, Biodegradation of petroleum as a source of ^{13}C-enriched carbon dioxide in the formation of carbonate cement: Chemical Geology, v. 65, p. 283–291.

Freyer, H.D., 1978, Degradation of products of organic matter in evaporites containing trapped atmospheric gases: Chemical Geology, v. 23, p. 293–307.

Gerling, P., Whiticar, M.J., and Faber, E., 1988, Extreme isotope fractionation of hydrocarbon gases in Permian salts: Organic Geochemistry, v. 13, p. 335–341.

Grishina, S., Dubessy, J., Kontorovich, A., and Pironon, J., 1992, Inclusions in salt beds resulting from thermal metamorphism by dolerite sills (eastern Siberia, Russia): European Journal of Mineralogy, v. 4, p. 1187–1202.

Grishina, S., Pironon, J., Mazurov, M., Goryainov, S., Pustilnikov, A., Fon-Der-Flaas, G., and Guerci, A., 1998, Organic inclusions in salt: Part 3. Oil and gas inclusions in Cambrian evaporite deposit from east Siberia: A contribution to the understanding of nitrogen generation in evaporites: Organic Geochemistry, v. 28, p. 297–310.

Mook, W.G., 2001, Estuaries and the sea, *in* Rozanski, K., et al., eds., Environmental isotopes in the hydrological cycle. Principles and applications, Volume III: Vienna, IAEA/UNESCO, p. 49–59.

Nesmelova, Z.N., and Travnikova, L.G., 1973, Radiogenic gases in ancient salt deposits: Geochemistry International, v. 10, p. 554–559.

Oremland, R.S., and Taylor, B.F., 1978, Sulfate reduction and methanogenesis in marine sediments: Geochimica et Cosmochimica Acta, v. 42, p. 209–214.

Pironon, J., Pagel, M., Lévêque, M., and Mogé, M., 1995, Organic inclusions in salt: Part I. Solid and liquid organic matter, carbon dioxide and nitrogen species in fluid inclusions from the Bresse basin (France): Organic Geochemistry, v. 23, p. 391–402.

Potter, J., and Siemann, M.G., 2004, A new method for determining $\delta^{13}C$ and δD simultaneously for CH_4 by gas chromatography/continuous flow–isotope ratio mass spectrometry: Rapid Communications in Mass Spectrometry, v. 18, p. 175–180.

Roedder, E., 1984, The fluids in salt: American Mineralogist, v. 69, p. 413–439.

Schoell, M., 1988, Multiple origins of CH_4 in the Earth: Chemical Geology, v. 71, p. 1–10.

Siemann, M.G., 2003, Extensive and rapid changes in seawater chemistry during the Phanerozoic: Evidence from Br contents in basal halite: Terra Nova, v. 15, p. 243–248.

Siemann, M., and Ellendorff, B., 2001, The composition of gases in fluid inclusions of Late Permian (Zechstein) marine evaporites in northern Germany: Chemical Geology, v. 173, p. 31–44.

Siemann, M.G., and Schramm, M., 2002, Henry's and non-Henry's law behavior of Br in simple marine systems: Geochimica et Cosmochimica Acta, v. 66, p. 1387–1399.

Sonnenfeld, P., 1984, Brines and evaporites: London, Academic Press, 613 p.

Stiller, M., Rounick, J.S., and Shasha, S., 1985, Extreme carbon-isotope enrichments in evaporating brines: Nature, v. 316, p. 434–435.

Whiticar, M.J., Faber, E., and Schoell, M., 1986, Biogenic methane formation in marine and freshwater environments: CO_2 reduction vs. acetate formation—Isotope evidence: Geochimica et Cosmochimica Acta, v. 50, p. 693–709.

Manuscript received 19 November 2003
Revised manuscript received 9 February 2004
Manuscript accepted 9 February 2004

Printed in USA